

Preparation of pH-sensitive CaP nanoparticles coated with a phosphate-based block copolymer for efficient gene delivery

Sangmok Jang^a, Seonju Lee^a, Heejin Kim^a, Jiyeon Ham^a, Ji-Hun Seo^b, Yeongbong Mok^a, Minwoo Noh^a, Yan Lee^{a,*}

^a Department of Chemistry, Seoul National University, 599 Gwanak-ro, Gwanak-gu, Seoul 151 747, Republic of Korea

^b Department of Organic Materials, Institute of Biomaterials and Bioengineering, Tokyo Medical and Dental University, 2-3-10 Kanda-Surugadai, Chiyoda, Tokyo 101-0062, Japan

ARTICLE INFO

Article history:

Received 20 June 2012

Received in revised form

14 August 2012

Accepted 18 August 2012

Available online 24 August 2012

Keywords:

Block copolymer
Calcium phosphate
pH-sensitivity

ABSTRACT

We have synthesized a phosphate-based block copolymer, PEG-*b*-PMOEP (poly(ethylene glycol)-*b*-poly(2-methacryloyloxyethyl phosphate)), with a narrow molecular weight distribution (PD = 1.06) by atomic transfer radical polymerization (ATRP), and have constructed calcium phosphate nanoparticles (CaPNs) coated with the block copolymer as an efficient and safe intracellular gene delivery carrier. The phosphate-mimic PMOEP block could be incorporated into the calcium phosphate (CaP) core to entrap pDNA, with the PEG block forming a shell to prevent uncontrolled growth of CaP precipitates and aggregates in physiological fluids. The CaPNs showed high colloidal stability at pH 7.4, but released entrapped pDNA at an endosomal pH of 5.0 through a pH-dependent protonation of phosphate moieties for efficient endosomal escape. The PEG-*b*-PMOEP/CaP/pDNA nanoparticles, which were formed simply by mixing, exhibited great potential as gene delivery carriers for future gene therapy applications due to their high transfection efficiency, low toxicity, and good stability under physiological conditions.

© 2012 Elsevier Ltd. All rights reserved.

1. Introduction

Calcium phosphate (CaP), the major component of bone, has been used as an important biomaterial for dental remodeling, tissue engineering, and drug delivery [1–3]. Due to the strong Coulombic interaction between calcium and phosphate ions that leads to hydration resistance, CaP has low aqueous solubility, an important characteristic for many of its applications. The addition of DNA to calcium and phosphate ions while forming CaP precipitates in aqueous solution allows the DNA to be incorporated as a co-precipitate. The CaP–DNA co-precipitate can be readily internalized into cells, and the entrapped DNA released into the cytosol, a phenomenon that has been recognized as an effective method for intracellular gene delivery since the 1960s [4,5].

As the concept of gene therapy through delivery of nucleic acid drugs into cells has evolved as potential cures of human diseases, various non-viral gene delivery methods have been developed including polymer–DNA complexes (polyplex) [6,7], lipid–DNA complex (lipoplex) [8,9], and electroporation [10,11] due to the potential dangers of viral gene delivery methods [12,13]. Because the efficiency and safety of developed non-viral gene delivery

methods for applications in human gene therapy are still unsatisfactory, only a small number of clinical trials have shown limited success [14]. Therefore, research into the development of efficient and safe gene delivery carriers is on-going, and the CaP co-precipitation method has been revived as an important and reliable delivery device candidate due to its efficiency, biocompatibility, bioresorbability, and simple preparation. However, the uncontrolled growth and rapid decrease of physiological stability of CaP precipitates significantly limits their application as gene delivery carriers in biological systems. Large aggregates over several micrometers in diameter cannot be easily internalized into cells via the endocytic process [15], and can also block the blood stream in fine capillaries [16,17]. Additionally, the accumulation of large aggregates in organs such as the lungs, skin, or intestines can significantly reduce delivery efficiency and specificity [16].

In order to control the growth and to improve the physiological stability of CaP precipitates with reproducible physicochemical characteristics that provide gene delivery with greater efficiency and safety, lipids and polymers have been used as detergents and coating materials. However, the process of preparing CaP micro- or nanoparticle emulsions in the presence of lipids [18] or polymers [19] requires relatively complex steps that include sonication or homogenization, which can damage DNA due to shearing forces. Alternatively, CaP nanoparticles can be efficiently prepared by the simple addition of a block copolymer during the co-precipitation

* Corresponding author. Tel.: +82 2 880 4344; fax: +82 2 871 2496.
E-mail address: gacn@snu.ac.kr (Y. Lee).

process. If a block copolymer with a neutral hydrophilic block (e.g. poly(ethylene glycol) (PEG)) and a negatively charged block (e.g. poly(aspartic acid) (PAA)) is added to the calcium phosphate solution, the negatively charged block can be incorporated into the core of the CaP precipitate through interactions between the calcium ions and negatively charged moieties, and the neutral hydrophilic block can form a shell to prevent uncontrolled aggregation through steric repulsion [20–23].

In this study, we synthesized PEG-*b*-PMOEP (poly(ethylene glycol)-*b*-poly(2-methacryloyloxyethyl phosphate)) with a narrow molecular weight distribution (PD = 1.06) by atomic transfer radical polymerization (ATRP), then prepared pDNA-encapsulated CaP nanoparticles (CaPNs) by coating with the PEG-*b*-PMOEP, and measured the enhancement of gene delivery efficiency with the nanocarrier. The PMOEP block, which resembles the head group of phosphatidic acid (PA), has many phosphomonoester moieties that strongly interact with calcium ions forming the CaP core, and the PEG block with a sufficient length ($M_n = 5000$) forms a hydrophilic shell that can control the size of the CaP particle to approximately 200 nm (Fig. 1). Phosphomonoester moieties have two distinct pK_a values, $pK_{a1} = \sim 3$ and $pK_{a2} = \sim 7$ [24] unlike carboxylate moieties

with pK_a of ~ 4 . It was expected that doubly charged phosphomonoester moieties could stabilize CaP nanoparticles at neutral pH via strong interaction with calcium ions, whereas the CaP nanoparticles could be destabilized by gradual protonation of the phosphomonoester moieties during the acidification in the early endosome allowing release of encapsulated nucleic acids. The enhancement of gene delivery efficiency by the phosphate-based polymer coating was analyzed by comparison with non-coated CaP precipitates and other gene delivery methods.

2. Experimental

2.1. Materials

Poly(ethylene glycol) mono-methyl ether (PEG-OH; $M_n = 5000$, $M_w = 5300$), 2-bromoisobutyryl bromide, triethylamine (TEA), 2-hydroxyethyl methacrylate (HEMA), dimethyl chlorophosphate (DCP), copper (I) bromide (CuBr), 2,2'-bipyridine (Bpy), trimethylsilyl bromide (TMSBr), calcium chloride (CaCl_2), 4-(2-hydroxyethyl)-1-piperazineethanesulfonic acid (HEPES), and 3-[4,5-dimethylthiazol-2-yl]-2,5-diphenyltetrazolium bromide (MTT)

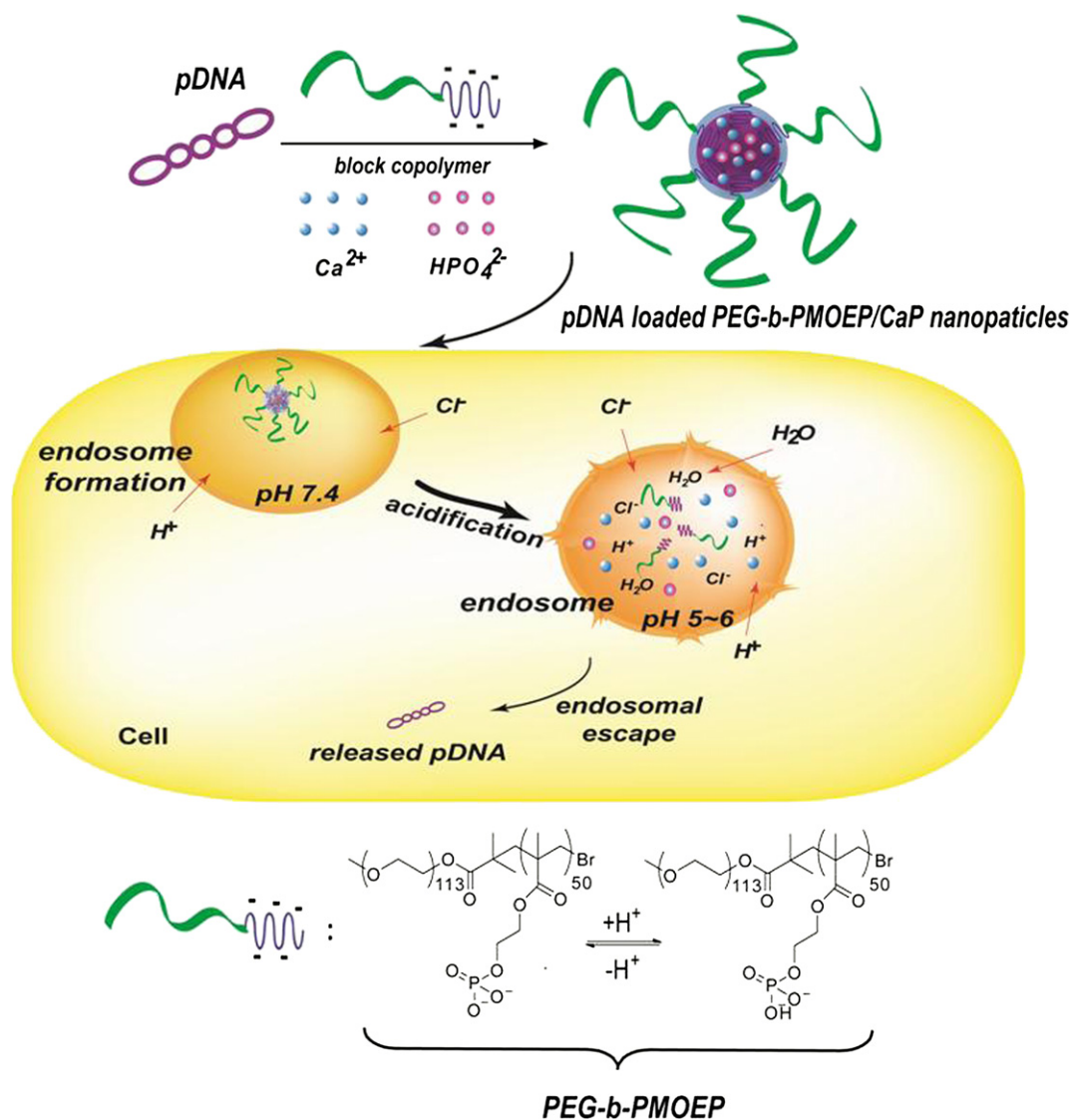


Fig. 1. Preparation of pDNA loaded PEG-*b*-PMOEP/CaP nanoparticles and its proposed release process to the endosome after endocytosis for gene delivery.

were purchased from Sigma–Aldrich (St. Louis, MO, USA). Methanol (MeOH), chloroform, and methylene chloride (MC) were purchased from Daejung (South Korea). The luciferase assay system and reporter lysis buffer were purchased from Promega (Madison, WI, USA). Dulbecco's Modified Eagle's Medium (DMEM), trypsin-EDTA, 100 × antibiotic–antimycotic (penicillin, streptomycin, and amphotericin B), and fetal bovine serum (FBS) were purchased from GIBCO (Gaithersburg, MD, USA). Phosphate-buffered saline (PBS) was purchased from Cambrex Bio Science (Walkersville, MD, USA). All chemicals were used without further purification. The Micro BCA™ Protein Assay Kit was purchased from Pierce (Rockford, IL, USA). A firefly luciferase expression plasmid, pCN-Luci, was constructed by subcloning the cDNA of *Photinus pyralis* luciferase with the 21 amino acid nuclear localization signal of SV40 large T antigen into pCN plasmids.

ExGen 500 was purchased from Fermentas (Burlington, Ontario, Canada).

2.2. Synthesis of PEG macroinitiator (**3**)

PEG-OH (**1**) (2.0 g, 0.40 mmol) and TEA (390 μL, 2.8 mmol) were dissolved in 14 mL of MC. After cooling the solution with an ice bath, 2-bromoisobutyryl bromide (**2**) (500 μL, 4.0 mmol) was slowly added to the vigorously stirred solution. The solution was further stirred at room temperature for 24 h. The resulting PEG macroinitiator (**3**) could be purified by precipitation in diethyl ether (yield > 90%). The MALDI-TOF MS (Bruker Daltonics, Bremen, Germany) spectra of **1** and **3** are shown in Figure S1.

2.3. Synthesis of MPDME (2-methacryloyloxyethyl phosphoryldimethylester) monomer (**4**)

HEMA (4.85 mL, 40.0 mmol) and pyridine (3.22 mL, 40.0 mmol) were dissolved in 15 mL of chloroform. DCP (15.7 mL, 120 mmol) was added dropwise to the ice-cold solution under stirring. After stirring at room temperature for 48 h, the reaction mixture was diluted with chloroform (35 mL). The solution was then extracted with 100 mL of 0.1 N HCl, and the organic layer was collected, dried over MgSO₄, and concentrated by rotary evaporation to yield MPDME (**4**).

¹H NMR (300 MHz, CDCl₃, δ ppm): δ1.93 (3H, CH₂=CCH₃CO₂-), δ3.80–4.00 (6H, -(CH₂)₂OPO(OCH₃)₂), δ4.20–4.50 (4H, -CO₂(CH₂)₂OPO-), δ5.90–6.10 (2H, CH₂=CCH₃CO₂-).

2.4. Synthesis of PEG-*b*-PMPDME (PEG-*block*-poly(2-methacryloyloxyethyl phosphoryldimethylester)) (**5**)

PEG₁₁₃-*b*-PMPDME₅₀ (**5**) was synthesized by ATRP using **3** as a PEG₁₁₃-Br macroinitiator. **3** (0.20 g, 0.039 mmol) was added to a solution of MPDME (460 μL, 2.0 mmol) in MeOH (4 mL). After three freeze–pump–thaw cycles, dried CuBr (12 mg, 0.078 mmol) and bpy (24 mg, 0.16 mmol) were added to the solution under an argon atmosphere. Polymerization was carried out at 40 °C for 12 h. After polymerization was complete, the solution was poured into excess ether to precipitate the product. **5** was obtained by drying the precipitate under vacuum (yield > 90%). The polymerization efficiency from **3** was almost 99%. The ¹H NMR spectrum of **5** is shown in Fig. 3(a). From the ¹H NMR spectrum, the degree of polymerization (DP) of PMPDME units was calculated to be 50.

2.5. Synthesis of PEG-*b*-PMOEP (PEG-*block*-poly(2-methacryloyloxyethyl phosphate)) (**6**)

PEG₁₁₃-*b*-PMPDME₅₀ (**5**) (190 mg) was added to a solution of TMSBr (290 μL, 2.2 mmol) in MC (10 mL) for deprotection of the

phosphoesters [25]. After stirring at 0 °C for 20 h, the solution was poured into excess ether to precipitate the product. After drying the product under vacuum, it was dissolved in MC (5 mL), and the solution was dialyzed against MeOH, and then against deionized water (M.W.C.O. = 6000–8000). The final product (**6**) was obtained by lyophilization (yield > 95%). From the ¹H NMR spectrum (Fig. 3(b)), the degree of polymerization (DP) of PMOEP units was calculated to be 50. The molecular weight distribution of PEG₁₁₃-*b*-PMOEP₅₀ was determined by gel permeation chromatography (GPC) using a Superdex™ 75 column (GE healthcare, USA) calibrated by PEG standards. 50 mM Tris–HCl (pH 7.4) was used as the eluent at a flow rate of 0.7 mL/min at 35 °C.

2.6. PEG-*b*-PMOEP/CaP/pDNA nanoparticle preparation

A solution of 2.5 M CaCl₂ was added to a solution of pCN-Luci DNA in distilled water to prepare a 2 × stock solution (Ca²⁺ 250 mM, pCN-Luci DNA 10 μg/mL). An aliquot of the stock solution was quickly added to an equal volume of 2 × PEG-*b*-PMOEP/phosphate solution (pH 7.1, 50 mM HEPES, 6.0 mM Na₂HPO₄, 300 mM NaCl). After vigorous mixing for a few seconds, the mixture was incubated at 47 °C for 24 h. The size distribution and zeta potential of nanoparticles in the suspension was analyzed at 37 °C by dynamic light scattering using a Zetasizer 3500 (Malvern Instruments, USA) equipped with a He–Ne ion laser at a wavelength of 633 nm.

2.7. Measurement of pCN-Luci DNA entrapment efficiency

After the formation of PEG-*b*-PMOEP/CaP/pDNA nanoparticles, the sample suspension was centrifuged at 15,000 × g for 30 min to precipitate the nanoparticles. The pCN-Luci DNA concentration in the supernatant was calculated from the absorbance at 260 nm. Entrapment efficiency (%EE) was determined using the following equation:

$$\%EE = \frac{[A]_0 - [A]_s}{[A]_0} \times 100$$

where [A]₀ and [A]_s are the OD values of the initial pDNA solution and the supernatant, respectively.

2.8. pH-Sensitive release of pCN-Luci DNA

The PEG-*b*-PMOEP/CaP/pDNA nanoparticle solution (PEG-*b*-PMOEP concentration = 500 μg/mL) was centrifuged at 13,000 × g for 10 min. The supernatant was carefully removed, and the precipitate was resuspended in two aqueous buffer solutions (pH 7.4 and pH 5.0). Each sample was dialyzed against buffer solution at 37 °C using a D-Tube dialyzer (M.W.C.O. = 6000–8000). Agarose gel electrophoresis on 1.0% (w/v) agarose gel was used for analysis of DNA release. After electrophoresis, the gel was stained with ethidium bromide solution (0.5 μg/mL), and the DNA band was visualized on a UV illuminator. The intensity of the DNA band was analyzed by a gel image analysis software (GelQuant.NET software, Biochemlabsolutions.com).

2.9. Cytotoxicity measurement

To determine the cytotoxicity of the nanoparticles, MTT assays were performed. HeLa cells were seeded in 96-well tissue culture dishes at 5000 cells/well in 90 μL of DMEM containing 10% FBS for 24 h before transfection. After replacing the medium with fresh complete medium, 30 μL of each sample was added and the cells were further incubated for 24 h. 20 μL of filtered MTT solution

(2 mg/mL in PBS) was added to each well. After incubation for 4 h at 37 °C, the medium was removed from the wells and 150 μ L of DMSO was added to dissolve the formazan crystals. Absorbance was measured at 570 nm using a microplate reader (Molecular Devices Co., Menlo Park, CA, USA) and cell viability was calculated by comparison with untreated control cells. Triplicate experiments were performed for determining the average value and standard deviation.

2.10. Cell culture and transfection

HeLa cells (human cervical cancer cells) were grown in complete medium (DMEM supplemented with 10% FBS and 1% antibiotics) at 37 °C in a humidified 5% CO₂ incubator. HeLa cells were seeded at a density of 15,000 cells/well into 24-well tissue culture dishes in 600 μ L of complete medium for 24 h before transfection. 120 μ L of all samples (pDNA only, CaP normal, CaPNs, ExGen 500) with complete medium (DMEM supplemented with 10% FBS and 1% antibiotics) were added to the cells at a final pCN-Luci DNA concentration of 0.5–4 μ g/mL and the cells were further incubated for 48 h.

For the transfection with ExGen 500, N/P ratio of 6 was used as an optimal transfection condition. For the luciferase assay, the growth medium was removed and the cells were washed with PBS and lysed for 30 min at room temperature with 150 μ L of reporter lysis buffer. Luciferase activity in the transfected cells was measured using an LB 9507 luminometer (Berthold, Germany) with 10 μ L of the lysate dispensed into a luminometer tube and the automatic injection of 50 μ L of Luciferase Assay Reagent. The protein concentration of the lysate was determined using a MicroTM BCA protein assay kit. Luciferase activity was measured in terms of relative light units (RLU) and the final values were determined as RLU/mg of total protein in the lysate. Triplicate experiments were performed for determining the average value and standard deviation. A *t*-test was performed between individual treatment groups, using the software Graphpad Prism 5.04 (GraphPad software, Inc.).

3. Results and discussion

3.1. Synthesis of PEG-*b*-PMOEP

ATRP is one of the most powerful methods to control the polymerization of a wide range of monomers [26]. In this study, a diblock copolymer with a neutral hydrophilic PEG block and a negatively charged phosphate block, PEG-*b*-PMOEP (**6**), was synthesized by ATRP (Fig. 2) to form a surface coating for CaP nanoparticles (CaPNs). The PEG macroinitiator, PEG-Br (**3**), was synthesized from PEG-OH (**1**) and 2-bromoisobutyryl bromide (**2**). Because it was difficult to determine the conjugation efficiency by ¹H NMR due to the relatively small number of terminal residues, MALDI-TOF was used as an alternative method to compare the molecular weight difference between **1** and **3**. Figure S1 shows that the conversion from **1** to **3** was almost 100% efficient. The phosphoryldimethylester monomer, MPDME (**4**), was prepared from HEMA and DCP since ATRP is often hampered by the presence of acid groups [27,28]. In addition, MPDME (**4**) was quite soluble in alcoholic ATRP solvents that were used to dissolve the PEG macroinitiator.

PEG-*b*-PMPDME (**5**) was synthesized from the PEG macroinitiator (**3**) using CuBr and bpy as the catalyst and ligand, respectively (Fig. 3(a)). PEG-*b*-PMOEP (**6**) was easily obtained through demethylation of **5**. After demethylation, proton peaks at δ 3.80–4.00 ppm corresponding to dimethyl esters of **5** had completely disappeared from the ¹H NMR spectrum (Fig. 3(b)). The molecular weight distribution of the product block polymer was analyzed by

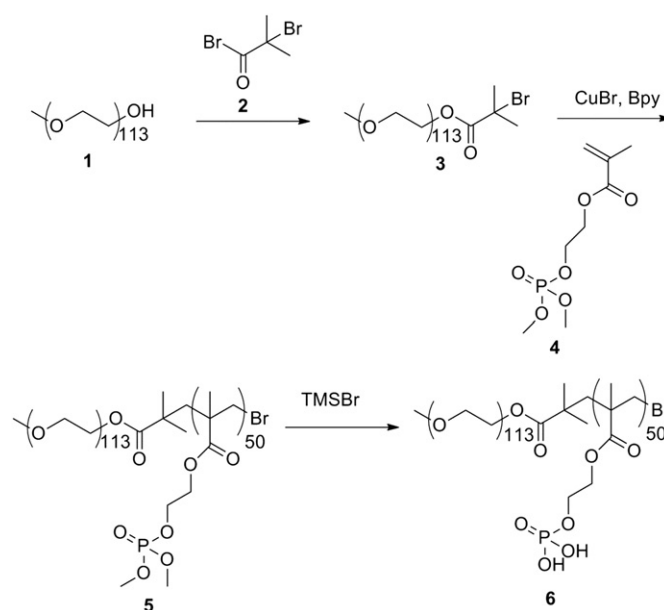


Fig. 2. Synthetic scheme of PEG-*b*-PMOEP (**6**) by ATRP.

both ¹H NMR and GPC (Table 1). From ¹H NMR, the degree of polymerization (DP) of the PMOEP block was calculated to be 50. The polydispersity (PD) of **6** was 1.06, which represents a successful ATRP of the phosphate-based block copolymer with a narrow molecular weight distribution.

3.2. Preparation of PEG-*b*-PMOEP/CaP/pDNA nanoparticles

The newly synthesized phosphate-based block copolymer, PEG-*b*-PMOEP, was used to prepare pDNA-encapsulated CaPNs for gene delivery. When calcium ions were mixed with phosphate ions, mixed salts including monocalcium phosphate (Ca(H₂PO₄)₂) and dicalcium phosphate (CaHPO₄) were formed depending on the pH of the solution. DNA could be readily incorporated into the CaP precipitates during the precipitation process. Growth of the precipitates was difficult to be controlled and very heterogeneous precipitates were formed without stabilizing reagents. In presence of PEG-*b*-PMOEP, the phosphate-based PMOEP block could be incorporated into the CaP precipitate core, and the neutral hydrophilic PEG block could coat the surface of the CaP. Because a PEG of short length is not sufficient for complete shielding and steric stabilization of nanoparticles to prevent protein–nanoparticle interactions in physiological fluids [29], we chose the PEG block with *M_n* = 5000 for stabilization of CaP particles.

pDNA-encapsulated CaP nanoparticles were simply prepared by mixing Ca²⁺/pDNA and phosphate/PEG-*b*-PMOEP solutions. The colloidal stability of CaPNs was highly dependent upon the concentration of the phosphate-based block copolymer. CaPNs less than 200 nm in diameter formed only with concentrations of the block copolymer over 380 μ g/mL (Fig. 4(a)). In the range of 400–500 μ g/mL, PEG-*b*-PMOEP/CaP/pDNA nanoparticles of approximately 180 nm in size were obtained. These CaPNs showed a unimodal size distribution with polydispersity indices (PDI) ranging from 0.1 to 0.2, which was confirmed by dynamic light scattering (DLS) analysis (Fig. 4(b–c)). The incubation temperature was another important factor for successful formation of PEG-*b*-PMOEP/CaP/pDNA nanoparticles. CaPNs with narrower size distributions were generally obtained as the temperature was increased (data not shown). Considering both narrow size distributions and

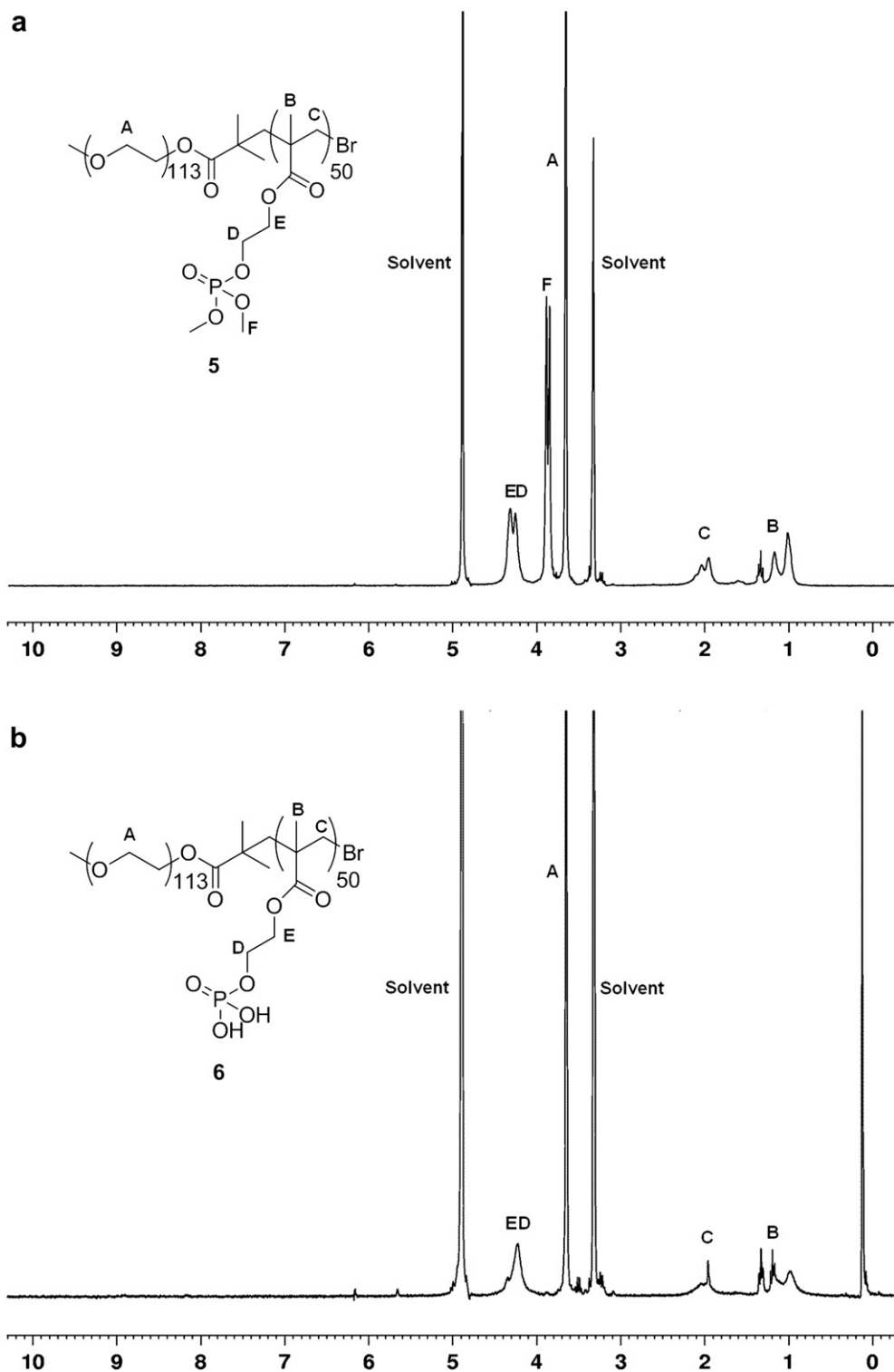


Fig. 3. ^1H NMR spectra of (a) PEG-*b*-PMPDME (**5**) and (b) PEG-*b*-PMOEP (**6**) in CD_3OD .

Table 1
Measurement of molecular weights of polymers.

	M_{n1}^a	M_{n2}^b	M_w^b	PD (M_w/M_n) ^b
PEG-Br initiator (3)	5.15×10^3	4.95×10^3	5.10×10^3	1.03
PEG- <i>b</i> -PMOEP (6)	1.56×10^4	1.72×10^4	1.82×10^4	1.06

^a The values are determined from ^1H NMR spectra.

^b The values are determined by GPC.

thermal denaturation of pDNA at higher temperatures, we determined the optimal temperature to be 47 °C for the transfection experiments shown below.

3.3. Measurement of entrapment efficiency and zeta potential

The entrapment efficiency of pDNA in the polymer-coated CaPNs was measured by UV absorbance at 260 nm. Fig. 5 shows

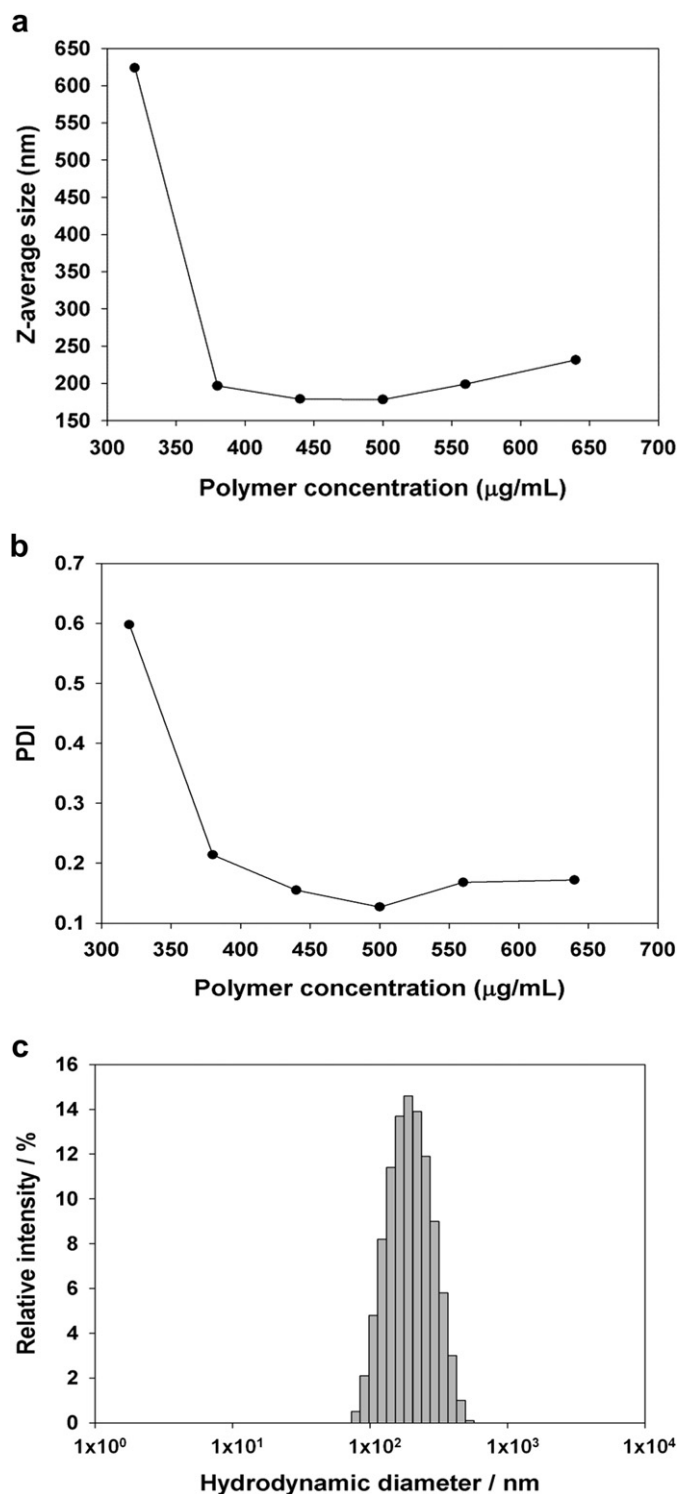


Fig. 4. Formation of PEG-*b*-PMOEP coated CaP nanoparticles with pDNA entrapment. (a) Polymer concentration dependence of the size of the CaP nanoparticles. (b) Polymer concentration dependence of the PDI of the CaP nanoparticles. (c) The sized distribution of the CaP nanoparticles (PEG-*b*-PMOEP concentration = 500 µg/mL). All data points are corresponding to CaP nanoparticles prepared at 47 °C.

the entrapment efficiency and zeta potential for three different PEG-*b*-PMOEP concentrations (0, 440, and 500 µg/mL). All samples had showed that more than 80% of the pDNA loaded into the CaP particles, which suggests that the pDNA incorporation efficiency was not closely related with the polymer coating but was affected by the co-precipitation process. However, the surface charges of

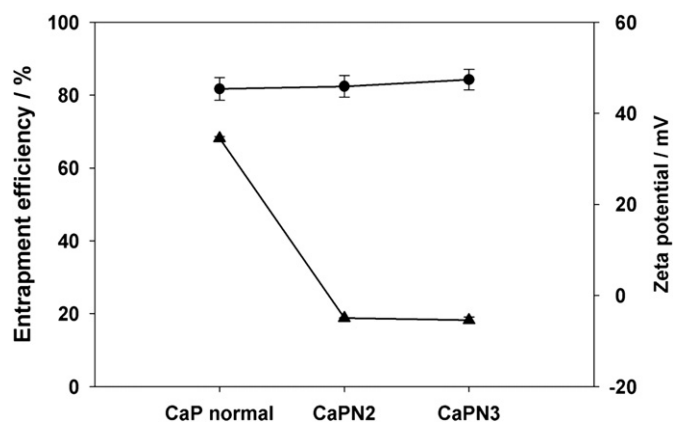


Fig. 5. Entrapment efficiency (●) and zeta potential (▲) of pDNA loaded PEG-*b*-PMOEP/CaP nanoparticles (PEG-*b*-PMOEP concentration of CaP normal, CaPN 2, CaPN 3 = 0, 440, 500 µg/mL, respectively). Error bars indicate the standard deviation ($n = 3$).

CaP particles were strongly dependent upon the polymer coating. CaP normal showed a zeta potential of about +33 mV, but polymer-coated CaPNs showed a zeta potential closed to zero, which suggested that neutral hydrophilic PEG block formed a shell on the surface of CaPNs.

3.4. pH-Sensitive release of DNA from PEG-*b*-PMOEP/CaP/pDNA nanoparticles

Because the electrostatic interaction between Ca^{2+} and H_2PO_4^- is weaker than between Ca^{2+} and HPO_4^{2-} , the aqueous solubility of CaP increases as the pH decreases [30]. It was also expected that the interaction between PEG-*b*-PMOEP and Ca^{2+} would decrease as a result of gradual protonation of phosphate groups in the PMOEP backbone.

Nanoparticles of several hundred nanometers in size are readily internalized into cells through the endocytic process, an important pathway for efficient intracellular drug/gene delivery [31]. Subsequently, internalized nanoparticles should escape the endosome into the cytosol before full acidification (pH 4) or maturation to a lysosome in which degrading enzymes are activated [32]. It was expected that the dissolution of CaP into calcium and phosphate ions at acidic pH can increase osmotic pressure in the endosome to induce endosomal membrane rupture by osmotic swelling and released pDNA from CaP can escape the endosome efficiently [33].

Therefore, release of pDNA from CaPNs at the endosomal pH 5.0 and normal physiological pH 7.4 were compared. Fig. 6 shows the result of agarose gel electrophoresis after incubation of PEG-*b*-PMOEP/CaP/pDNA nanoparticles at the two different pH values. At pH 7.4, no release of pDNA from the nanoparticles was detected even after 24 h and the nanoparticles maintained a narrow size distribution with high colloidal stability even after 72 h (data not shown). On the other hand, pDNA release began after 1 h at pH 5.0 with about 70% of the pDNA released from the CaPNs after 1 h and almost 95% released after 2 h as measured by a gel image analysis software. These results strongly support the supposition that PEG-*b*-PMOEP/CaP/pDNA nanoparticles can dissociate and the released pDNA can escape the endosome in the weakly acidic early endosomal state before degradation and inactivation of pDNA in the lysosome.

3.5. Cytotoxicity measurement of PEG-*b*-PMOEP and PEG-*b*-PMOEP/CaP/pDNA nanoparticles

Cytotoxicity of free PEG-*b*-PMOEP and CaPNs was measured separately by the MTT assay. Compared to ExGen 500 (linear

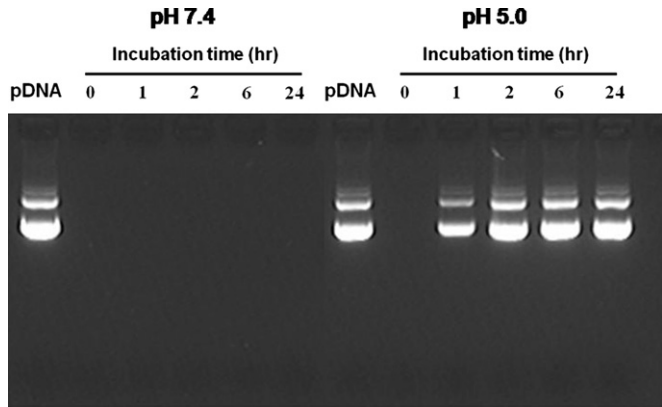


Fig. 6. pH-sensitive release of pDNA from PEG-*b*-PMOEP/CaP nanoparticles according to the incubation time on pH 7.4 and pH 5.0, respectively (PEG-*b*-PMOEP concentration = 500 $\mu\text{g}/\text{mL}$).

polyethylenimine), a commercially available transfection reagent, which showed about 20% of cell viability at the concentration of 10 $\mu\text{g}/\text{mL}$, free PEG-*b*-PMOEP showed almost no cytotoxicity even at the polymer concentration of 40 $\mu\text{g}/\text{mL}$ (Fig. 7(a)). Additionally, non-toxicity of PEG-*b*-PMOEP/CaP/pDNA nanoparticles (CaPN 2)

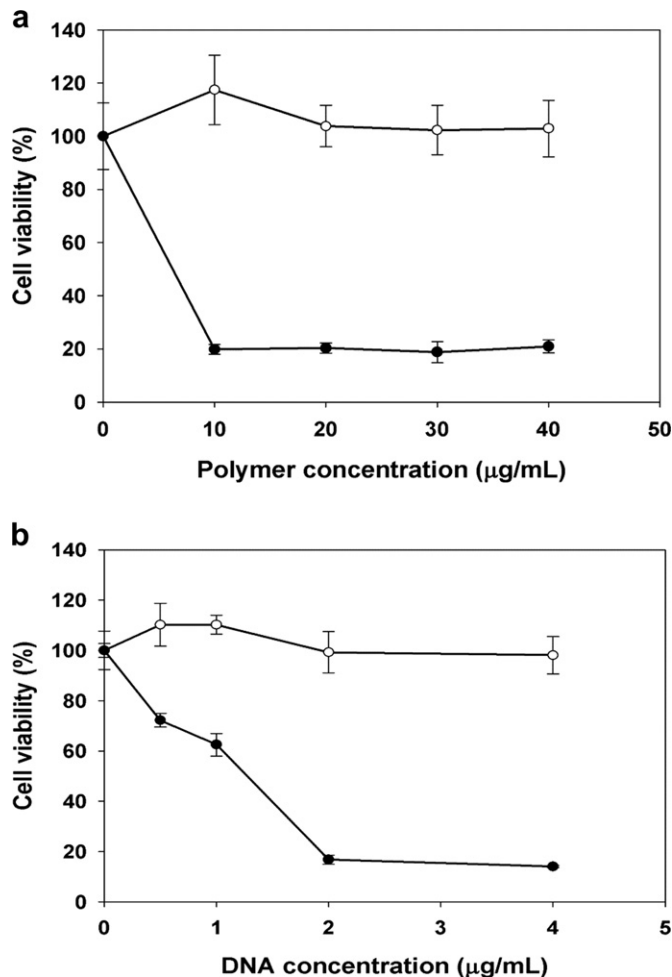


Fig. 7. (a) Cytotoxicity of PEG-*b*-PMOEP (\circ) and ExGen 500 (\bullet) at various polymer concentration on HeLa cells. (b) Cytotoxicity of CaPN 2 (\circ) and ExGen 500/pDNA polyplex (N/P = 6) (\bullet) at various pDNA concentration on HeLa cells. Error bars indicate the standard deviation ($n = 3$).

was also confirmed until the pDNA concentration of 4 $\mu\text{g}/\text{mL}$ (Fig. 7(b)). The cytotoxicity results support the potential of PEG-*b*-PMOEP/CaP/pDNA nanoparticles as safe gene delivery carriers for use in biosystems.

3.6. Transfection of HeLa cells by PEG-*b*-PMOEP/CaP/pDNA nanoparticles

Transfection experiments of HeLa cells were performed with PEG-*b*-PMOEP/CaP/pDNA nanoparticles. As shown in Fig. 8(a), the PEG-*b*-PMOEP-coated CaPNs showed about 2-fold higher transfection efficiency than normal CaP precipitates. By controlling the size of CaP precipitates to approximately 200 nm, the transfection efficiency could be significantly enhanced, probably due to more effective endocytic uptake of CaPNs compared to simple heterogeneous CaP precipitates with an average size over several micrometers [19]. As shown in confocal laser scanning microscopy (CLSM) images (Figure S2), normal CaP precipitates were difficult to be internalized into HeLa cells in spite of their positive surface charges, the PEG-*b*-PMOEP-coated CaPNs with almost neutral surface charges were efficiently internalized by endocytic pathways.

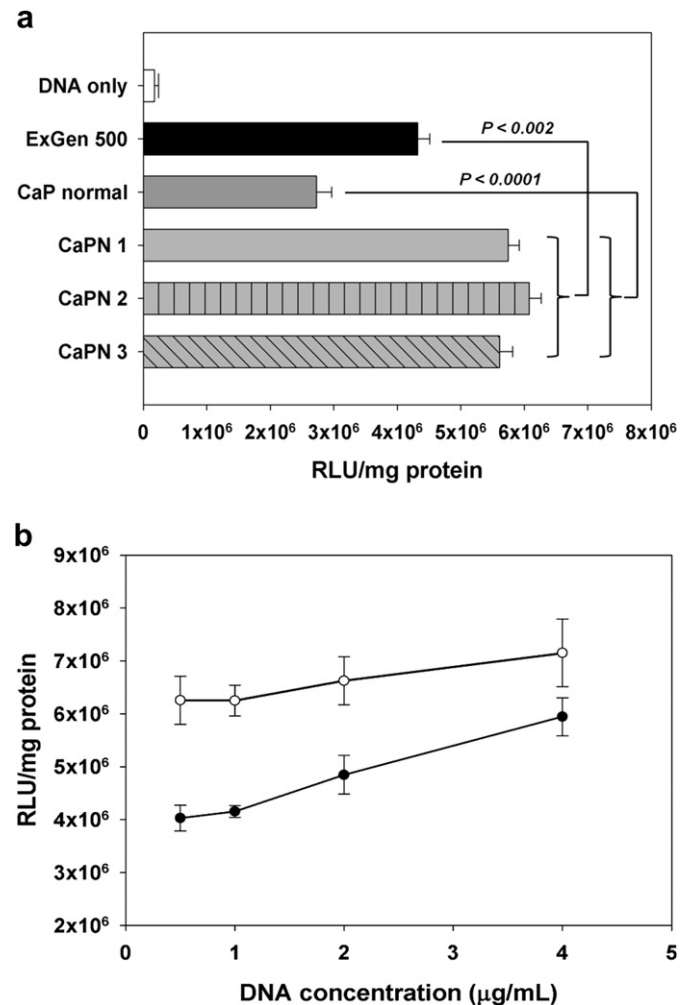


Fig. 8. (a) Transfection efficiency of PEG-*b*-PMOEP/CaP nanoparticles on HeLa cells at a pDNA concentration of 1.39 $\mu\text{g}/\text{mL}$ (PEG-*b*-PMOEP concentration of CaPN 1, CaPN 2, CaPN 3 = 380, 440, and 500 $\mu\text{g}/\text{mL}$, respectively). (b) Transfection efficiency of PEG-*b*-PMOEP/CaP nanoparticles (CaPN 2) (\circ) and ExGen 500 (N/P = 6) (\bullet) at various pDNA concentration on HeLa cells. Statistical significance was represented as *p* value. Error bars indicate the standard deviation ($n = 3$).

The effect of the initial PEG-*b*-PMOEP concentrations on transfection efficiency was negligible. For comparison with other non-viral gene delivery carriers, ExGen 500 was used as a positive control. Our CaPNs showed higher transfection efficiency compared to ExGen 500 at the pDNA concentration range of 0.5–4 µg/mL (Fig. 8(b)). The transfection efficiency of CaPNs and ExGen 500 polyplexes was gradually increased as the pDNA concentration was increased. It is probably due to increased uptake of CaPNs at higher pDNA concentrations.

Cationic polymer–pDNA complexes such as PEI–pDNA complex generally show high *in vitro* transfection efficiency due to their positive surface charges, however, they are difficult to apply to *in vivo* gene delivery due to the formation of large aggregates with negatively charged serum proteins [34]. Surface coating of the complexes with biocompatible hydrophilic polymers might be required to prevent such aggregation, but transfection efficiency is often reduced with a polymer coating [35]. Considering that the transfection efficiency of our PEG-*b*-PMOEP/CaP/pDNA nanoparticles was higher than that of the ExGen 500–pDNA complex even in the presence of a PEG shell, the CaPNs have great potential as *in vivo* gene delivery carriers with both high delivery efficiency and safety.

4. Conclusion

PEG-*b*-PMOEP coated CaP nanoparticles were prepared as carriers for the efficient intracellular delivery of pDNA. The phosphate-based block copolymer strongly interacts with calcium ions and prevents the uncontrolled growth of CaP precipitates. Simple addition of the phosphate-based polymer led to CaP nanoparticles being formed with an average size below 200 nm, a narrow size distribution, high pDNA entrapment efficiency, good colloidal stability at neutral pH, and allowed the selective release of the pDNA at weakly acidic pH. Compared to the uncoated CaP precipitate and ExGen 500, the PEG-*b*-PMOEP coated CaP nanoparticles exhibited great potential as efficient and safe gene delivery carriers for future gene therapy applications.

Acknowledgments

This work was supported by the Basic Science Research Program (2011-0002301) through the National Research Foundation (NRF) funded by the Ministry of Education, Science, and Technology of Korea and Seoul R&BD program (ST110017M0209721).

Appendix A. Supplementary material

Supplementary material associated with this article can be found, in the online version, at <http://dx.doi.org/10.1016/j.polymer.2012.08.043>.

References

- [1] Peter B, Pioletti DP, Laib S, Bujoli B, Pilet P, Janvier P, et al. *Bone* 2005;36:52–60.
- [2] Xie C, Lu H, Li W, Chen FM, Zhao YM. *J Mater Sci Mater Med* 2012;23:853–62.
- [3] Rosa V, Della Bona A, Cavalcanti BN, Nor JE. *Dent Mater* 2012;28:341–8.
- [4] Liu T, Tang A, Zhang GY, Chen YX, Zhang JY, Peng SS, et al. *Cancer Biother Radio* 2005;20:141–9.
- [5] Tabakovic A, Kester M, Adair JH. *Wires Nanomed Nanobiotechnol* 2012;4:96–112.
- [6] Boussif O, Lezoualc'h F, Zanta MA, Mergny MD, Scherman D, Demeneix B, et al. *Proc Natl Acad Sci* 1995;92:7297–301.
- [7] Lee Y, Miyata K, Oba M, Ishii T, Fukushima S, Han M, et al. *Angew Chem Int Ed* 2008;47:5163–6.
- [8] Zhou XH, Huang L. *BBA-Biomembranes* 1994;1189:195–203.
- [9] Ewert K, Slack NL, Ahmad A, Evans HM, Lin AJ, Samuel CE, et al. *Curr Med Chem* 2004;11:133–49.
- [10] Paquereau L, Le Cam A. *Anal Biochem* 1992;204:147–51.
- [11] Jaroszeski MJ, Gilbert R, Nicolau C, Heller R. *Adv Drug Delivery Rev* 1999;35:131–7.
- [12] Marshall E. *Science* 1999;286:2244–5.
- [13] Kaiser J. *Science* 2003;299:495.
- [14] Kwon MJ, An S, Choi S, Nam K, Jung HS, Yoon CS, et al. *J Gene Med* 2012;14:272–8.
- [15] Zhang SL, Li J, Lykotrafitis G, Bao G, Suresh S. *Adv Mater* 2009;21:419–24.
- [16] Lee Y, Kataoka K. *Adv Polym Sci* 2012;249:95–134.
- [17] Christie RJ, Nishiyama N, Kataoka K. *Endocr J* 2010;151:466–73.
- [18] Yang Y, Li J, Liu F, Huang L. *Mol Ther* 2012;20:609–15.
- [19] Roy I, Mitra S, Maitra A, Mozumdar S. *Int J Pharm* 2003;250:25–33.
- [20] Kakizawa Y, Kataoka K. *Langmuir* 2002;18:4539–43.
- [21] Kakizawa Y, Furukawa S, Kataoka K. *J Control Release* 2004;97:345–56.
- [22] Kakizawa Y, Furukawa S, Ishii A, Kataoka K. *J Control Release* 2006;111:368–70.
- [23] Pittella F, Zhang MZ, Lee Y, Kim HJ, Tockary T, Osada K, et al. *Biomaterials* 2011;32:3106–14.
- [24] Kooijman EE, Carter KM, van Laar EG, Chupin V, Burger KNJ, de Kruijff B. *Biochemistry* 2005;44:17007–15.
- [25] Sparrow JT, Monera OD. *J Pept Res* 1996;9:218–22.
- [26] Sant VP, Smith D, Leroux J-C. *J Control Release* 2004;97:301–12.
- [27] Zhou F, Huck WTS. *Chem Commun* 2005:5999–6001.
- [28] Suzuki S, Whittaker MR, Grondahl L, Monteiro MJ, Wentrup-Byrne E. *Bio-macromolecules* 2006;7:3178–87.
- [29] Wang G, Uludag H. *Expert Opin Drug Deliv* 2008;5:499–515.
- [30] Dorozhkin SV. *World J Methodol* 2012;2:1–17.
- [31] Khalil IA, Kogure K, Akita H, Harashima H. *Pharmacol Rev* 2006;58:32–45.
- [32] Breunig M, Bauer S, Goeffrich A. *Eur J Pharm Biopharm* 2008;68:112–28.
- [33] Bisht S, Bhakta G, Mitra S, Maitra A. *Int J Pharm* 2005;288:157–68.
- [34] van Gaal EVB, van Eijk R, Oosting RS, Kok RJ, Hennink WE, Crommelin DJA, et al. *J Control Release* 2011;154:218–32.
- [35] Papanicolaou I, Briggs S, Alpar HO. *J Drug Target* 2004;12:541–7.